Hong I, Garrett A, Maker G, Mullaney I, Rodger J, Etherington SJ. 2018. Repetitive low intensity magnetic field stimulation in a neuronal cell line: a metabolomics study. PeerJ 6:e4501
https://doi.org/10.7717/peerj.4501

Repetitive low intensity magnetic field stimulation in a neuronal cell line: A metabolomics study

Ivan Hong [1] , **Andrew Garrett** [2] , **Garth Maker** [1] , **Ian Mullaney** [1] , **Jennifer Rodger** [Corresp., 2, 3] , **Sarah J Etherington** [1]

[1] School of Veterinary and Life Sciences, Murdoch University, Murdoch, WA, Australia

[2] School of Biological Sciences, Experimental and Regenerative Neuroscience, The University of Western Australia, Crawley, WA, Australia

[3] Brain Plasticity laboratory, Perron Institute for Translational Neuroscience, Perth, WA, Australia

Corresponding Author: Jennifer Rodger
Email address: jennifer.rodger@uwa.edu.au

Low intensity repetitive magnetic stimulation of neural tissue modulates neuronal excitability and has promising therapeutic potential in the treatment of neurological disorders. However, the underpinning cellular and biochemical mechanisms remain poorly understood. This study investigates the behavioural effects of low intensity repetitive magnetic stimulation (LI-rMS) at a cellular and biochemical level. We delivered LI-rMS (10 mT) at 1 Hz and 10 Hz (n=5 wells per group) to B50 rat neuroblastoma cells *in vitro* for 10 minutes and measured levels of selected metabolites immediately after stimulation. LI-rMS at both frequencies depleted selected tricarboxylic acid (TCA) cycle metabolites without affecting the main energy supplies. Furthermore, LI-rMS effects were frequency-specific with 1 Hz stimulation having stronger effects than 10 Hz. The observed depletion of metabolites was consistent with an increase in GABA release as a result of higher spontaneous activity. Although the absence of organised neural circuits and other cellular contributors (e.g. excitatory neurons and glia) in the B50 cell line limits the degree to which our results can be extrapolated to the human brain, the changes we describe provide novel insights into how LI-rMS modulates neural tissue.

Repetitive Low intensity magnetic field stimulation in a neuronal cell line: a metabolomics study

Ivan Hong [1,2], Andrew Garrett [2], Garth Maker [1], Ian Mullaney [1], Jennifer Rodger [2,3], Sarah J. Etherington[1]

1. School of Veterinary and Life Sciences, Murdoch University, Murdoch WA.

2. Experimental and Regenerative Neuroscience, School of Animal Biology, University of Western Australia, Crawley WA.

3. Perron Institute for Neurological and Translational Science, Nedlands, WA

Corresponding author:

Dr Jennifer Rodger
Experimental and Regenerative Neuroscience,
School of Animal Biology, University of Western Australia.
35 Stirling Highway
Crawley 6009
Australia
Email: Jennifer.rodger@uwa.edu.au
Tel: (+61) 8 6488 2245

Abstract

Low intensity repetitive magnetic stimulation of neural tissue modulates neuronal excitability and has promising therapeutic potential in the treatment of neurological disorders. However, the underpinning cellular and biochemical mechanisms remain poorly understood. This study investigates the behavioural effects of low intensity repetitive magnetic stimulation (LI-rMS) at a cellular and biochemical level. We delivered LI-rMS (10 mT) at 1 Hz and 10 Hz (n=5 wells per group) to B50 rat neuroblastoma cells *in vitro* for 10 minutes and measured levels of selected metabolites immediately after stimulation. LI-rMS at both frequencies depleted selected tricarboxylic acid (TCA) cycle metabolites without affecting the main energy supplies. Furthermore, LI-rMS effects were frequency-specific with 1 Hz stimulation having stronger effects than 10 Hz. The observed depletion of metabolites was consistent with an increase in GABA release as a result of higher spontaneous activity. Although the absence of organised neural circuits and other cellular contributors (e.g. excitatory neurons and glia) in the B50 cell line limits the degree to which our results can be extrapolated to the human brain, the changes we describe provide novel insights into how LI-rMS modulates neural tissue.

Key words: rTMS, ELF-MF, GABA, neuron

Introduction

Faraday's discovery that a changing magnetic field induces a current in a conductor has contributed to many applications, such as the electromagnetic stimulation of body tissues and organs [Barker et al., 1985]. Specifically, electromagnetic stimulation of brain tissue has significant experimental and therapeutic potential because the induction of electric currents within neurons can modulate neuronal excitability, allowing non-invasive investigation and manipulation of brain circuit function and connectivity. Although clinical applications of magnetic fields most commonly involve high intensity fields that trigger action potentials and activate neural circuits [Müller-Dahlhaus and Vlachos, 2013], therapeutic effects are also observed during low intensity magnetic stimulation [Di Lazzaro et al., 2013; Rohan et al., 2014]. For example in humans, low intensity repetitive transcranial magnetic stimulation (LI-rTMS; pulse amplitude <100 mT) is beneficial in treating depression [Martiny et al., 2010] and pain [Shupak et al., 2004] and influences memory [Navarro et al., 2016].

It is apparent, however, that cellular mechanisms underpinning behavioural effects of LI-rTMS remain poorly characterised. Many studies in non-neuronal tissues and cells have focussed on the potentially negative effects of low intensity electromagnetic fields in the context of safety concerns surrounding the use of equipment emitting extremely low-frequency magnetic fields (ELF-MF; e.g. [ICNIRP, 1998]). However minimal investigation into low intensity stimulation in neuronal systems has been performed, despite demonstrated evidence of modulation of brain excitability in humans [Capone et al., 2009] and in animal models [Yang et al., 2015; Balassa et al., 2013]. It has been established that the intensity of the induced electric fields in LI-rTMS is not sufficient to depolarise neurons to action potential firing threshold [Davey and Riehl, 2006; Rudiak and Marg, 1994]. In contrast, *in vitro* experiments have consistently shown that low intensity repetitive magnetic stimulation (LI-rMS– no cranium) modulates intracellular calcium

levels in non-neuronal [Aldinucci et al., 2000; Walleczek and Budinger, 1992; Zhang et al., 2010] and neuronal cells [Grehl et al., 2015].

We recently demonstrated that LI-rMS of dissociated cortical neurons rapidly increases levels of intracellular calcium (within 10 minutes of the onset of stimulation), with higher levels of intracellular calcium detected following 10 Hz compared to 1 Hz stimulation [Grehl et al., 2015]. Such modulation of intracellular calcium alters NMDA receptor function [Manikonda et al., 2007] and provides a potential trigger for a wide range of changes in neuronal biochemistry which may underpin the LI-rTMS effects observed clinically [Martiny et al., 2010; Shupak et al., 2004]. Further, there is also evidence that low intensity magnetic fields alter levels of biochemicals that function in neuronal processes, for example, low intensity magnetic fields modulate the level of the primary metabolite of serotonin, 5-HIAA, in rat brain in a dose (time)-dependent manner [Shahbazi-Gahrouei et al., 2016]. In light of these findings, further investigation of biochemical and metabolic changes induced by LI-rMS in neuronal cells is warranted.

We hypothesize that changes in biochemical pathways due to LI-rTMS, will modify levels of a range of small molecule metabolites, including amino acids, carbohydrates and organic acids, which can be profiled using metabolomic techniques. Metabolomic analysis that profiles as many metabolites as possible in a single analysis is known as non-targeted screening. We performed such screening of a neuronal cell line immediately following 10 minutes of LI-rMS at 1 Hz or 10 Hz *in vitro*. We describe changes in the levels of 12 metabolites, 3 of which changed in a frequency-dependent manner.

METHODS

Cell culture

Rat neuroblastoma cells from the B50 cell line were seeded directly onto 6-well plates and grown for 24 hours in media containing DMEM with 5% (v/v) heat-inactivated foetal calf serum, 2mM L-glutamine, 100U/ml streptomycin and 100U/ml penicillin. Cells were grown at 37°C within a CO_2 incubator (5% CO_2 + 95% air). Cells from each 6-well plate were later pooled during extraction to make one replicate. Each stimulus condition or control had 6 replicates in total.

LI-rMS stimulation

We used LI-rMS parameters that have previously been shown to increase intracellular calcium in primary cultured neurons *in vitro [Grehl et al., 2015]*. Stimulation was delivered to cells in the incubator using custom built round coils (34 mm diameter, 17.1 mm height, 0.812 mm thickness, 138 turns). In order to deliver reproducible stimulation to each well, coils were designed to fit within a single well of a 6-well plate so that a plate containing cells could be placed on top of a plate containing 5 coils, resulting in reliable and reproducible placement at a distance of 2.8 mm from the base of each well (Figure. 1A,B). As the stimulator could only accommodate 5 coils, only 5 wells were stimulated on each plate. The coils were driven by a 12 V magnetic pulse generator under control of a programmable micro-controller card (CardLogix, USA), which delivered monophasic pulses (rise time of 0.725 ms). To approximate the stimulation dose in the 6-well plate, we measured the magnitude of the magnetic field in the x and y axes with a Hall Effect probe (Honeywell SS94A2D, USA). Magnetic field measurements were made at a distance of 0.5 cm from the base of the coil surface. Magnetic field strengths were converted to dB/dT, as a measure of the change in magnetic field over time of each delivered pulse. A map of dB/dT across the 6-well plate was generated with Matlab 2013a (Figure 1C). Peak magnetic field and dB/dT inside each well ranged between ~2.2 to ~2.4 mT and ~3 to ~3.2 T/s respectively. Coil

temperature did not rise above 37°C, ruling out confounding effects of temperature change. Vibration of the coil was assumed to be within vibration amplitude of background (bench surface), as shown previously in Grehl et al.[2015]. For the experiments, 6-well plates were assigned to one of 3 conditions: control (pulse generator switched off, no LI-rMS), 1 Hz (continuous stimulation for 10 minutes at 1 Hz) and 10 Hz (continuous stimulation for 10 minutes at 10 Hz). Stimulation and sham (control) stimulations were performed at 37°C within the CO_2 incubator.

Metabolite extraction and derivatisation

Cells were immediately quenched and washed twice post-stimulation with 2 ml of ice-cold phosphate-buffered saline. Cells were then scraped, aggregated and frozen in liquid nitrogen before being freeze-dried. 500 µl of extraction solution consisting of 2.6µg/ml of $^{13}C_6$-sorbitol, as an internal standard, was dissolved in methanol and added to the dried cells. Cells were lysed with a Precellys 24 tissue lyser (Bertin Technologies, France) at 6500rpm for 40 seconds. The supernatant was evaporated before adding 500 µl of water and freeze-drying again. Samples were derivatised according to the protocol described in Abbiset al.[2012]. 20µl of methoxyamine HCl solution (20mg/ml in pyridine) was added to each extract and agitated at 1200rpm and 30°C for 90 minutes. 40µl of N-methyl-N-(trimethylsilyl) trifluoroacetamide (MSTFA) was subsequently added to each extract and agitated at 300rpm and 37°C for 30 minutes. The derivatised samples were transferred to GC vials and 5 µl of alkanes(C_{10}, C_{12}, C_{15}, C_{19}, C_{22}, C_{28}; 0.156 mg.mL^{-1}; C_{32}, C_{36}; 0.313 mg/ml) in hexane were added to each sample for calculation of a Kovat's retention index, which aids comparison of data between samples.

Sample analysis

An Agilent 6890 series gas chromatograph with an Agilent 7863 autosampler coupled to an Agilent 5973N single quadrupole gas chromatography-mass spectrometer(GC-MS) (Agilent Technologies, Australia, Mulgrave, Australia) was used along with a Varian Factor Four-fused silica capillary column VF-5ms (30mx0.25mm x 0.25µm + 10m EZ-Guard). The analytical method was also as described in Abbisset al.[2012].1 µl of the sample was injected splitless into the inlet that was set to 230°C. The oventemperature was initially set to 70°C with an initial temperature ramp of 1°C/min for 5 minutes and was subsequently set to 5.63°C/min, to a final temperature of 330°C and held for 10 minutes. The ion source was set to 70 eV and 230°C while the transfer line to the mass spectrometer was set to 330°C. The detector, set to full scan, monitored a mass range of *m/z* 45-600 at 1 scan per second. The carrier gas, helium, was set at a flow rate of 1ml/min.

Data Analysis

Due to co-elution, the peaks of the $^{13}C_6$-sorbitol internal standard and glutamate could not be deconvoluted. Results were therefore normalized using the total ion chromatogram (TIC). The presence of aberrant peaks suggested that two of the 6-well plates (1 Hz stimulation condition) were not adequately washed during the extraction process and these were therefore excluded from the final analysis.

GC-MS data were viewed with AnalyzerPro v2.70 (SpectralWorks, Runcorn, UK). The mass spectra of peaks from the chromatogram were matched against the NIST (National Institute of Standards and Technology) mass spectral library. Metabolites with a similarity index of more than 60% were tentatively identified as metabolites. Metabolites with multiple derivative peaks were summed and treated as a single metabolite. Peak areas were normalised to the total ion

chromatogram (TIC) and imported into Unscrambler X version 10.1 (CAMO Software, Oslo, Norway). The data was log transformed [X=log(x+1)] and a principal component analysis (PCA) was performed using a non-iterative partial least squares algorithm, cross validation and no rotation. Statistical comparisons between treatment samples were conducted with SPSS v21 (IBM, Corporation, Armonk, USA) using a one-way ANOVA with Tukey's post-hoc test.

RESULTS

Based on GC-MS profiling, a total of 18 reproducible intracellular metabolites were identified from the total ion chromatograms (TIC) (Table 1). At 1 Hz, significant decreases were observed in a total of 12 metabolites. This included 7 amino acids, namely alanine, glycine, isoleucine, phenylalanine, serine, threonine (all $p < 0.01$) and aspartate (all $p < 0.05$). Significant decreases were also observed in cholesterol, glycylglutamic acid, inositol, pyroglutamate and succinate (all $p < 0.01$). Non-significant decreases were observed in three carbohydrates: fructose, galactose and glucose.

At 10 Hz, significant decreases were observed in a total of 9 metabolites, all of which were also significantly decreased at 1 Hz. These were the amino acids glycine, phenylalanine (both $p < 0.01$), isoleucine, serine and threonine (all $p < 0.05$), as well as glycylglutamic acid ($p < 0.01$), cholesterol, pyroglutamate and succinate (all $p < 0.05$). Non-significant decreases were also observed in the same three carbohydrates as for 1 Hz. Measured as a fold change, the decrease observed at 1 Hz was greater than at 10 Hz for all 12 significantly different metabolites.

In order to visualise the metabolomic data, relative peak areas (as measured by GC-MS) were subjected to principal component analysis (PCA). The PCA scores plot could be separated into 3 groups based on the frequency at which the cells were stimulated (Figure 2). The majority of the variation between control, 1 Hz and 10 Hz could be attributed to principal component 1 (PC-1), which accounted for 63% of the variance.

DISCUSSION

This study demonstrates for the first time that *in vitro* application of LI-rTMS depletes selected metabolites in B50 cells, including numerous amino acids. Furthermore, we confirm that LI-rMS effects are frequency-specific with 1 Hz stimulation having stronger effects than 10 Hz.

LI-rTMS induces specific metabolic changes associated with GABA synthesis

Following LI-rTMS, we did not detect any significant change in the levels of glucose, fructose or galactose, which are key energy supplies to the cell. This is in contrast with outcomes of high intensity rTMS in human and in cat studies, where changes in glucose levels were detected during and immediately after stimulation [Valero-Cabré et al., 2007]. In the latter studies, glucose uptake was significantly reduced during stimulation, suggesting a local suppression of neuronal firing [Valero-Cabré et al., 2007]. However, immediately after high frequency, high intensity rTMS, the same regions had increased metabolism [Valero-Cabré et al., 2005], presumably due to long lasting plastic changes in intracortical circuitry [Walsh and Pascual-Leone, 2003]. Together, these findings suggest that the intensity and frequency of stimulation contribute to changes in metabolic response.

However, in contrast to the stability of major carbohydrates, the metabolic profiles of metabolites implicated in GABA synthesis were reduced following LI-rMS. GABA is synthesised via glutamate, from α-ketoglutarate, a principal component of the TCA cycle (Figure 3, box a). We observed depletion of three amino acids involved in *de novo* synthesis of TCA cycle intermediates, aspartate, phenylalanine and isoleucine (see Figure 3, boxes b, c and d, respectively). A possible explanation is that LI-rMS caused increased spontaneous neurotransmitter release in B50 cells, requiring the use of α-ketoglutarate to replenish GABA pools and depleting the downstream TCA cycle intermediates and their substrates (Table 1 and

yellow boxes, Figure 3). Similarly, increased GABA synthesis could explain the LI-rTMS dependent reduction in pyroglutamate and alanine [Kumar and Bachhawat, 2012; Westergaard et al., 1993], both of which can be converted to glutamate and subsequently to GABA. In support of this, spontaneous transmitter release is increased following LI-rMS in excitatory neurons [Ahmed and Wieraszko, 2008], and our results suggest a similar increase in spontaneous GABA release from B50 cells.

Reduction in other amino acids and metabolites

The amino acids serine and glycine were also significantly decreased following 1 Hz and 10Hz LI-rMS. The technique used in our study could not differentiate between L- and D-serine. Although both stereoisomers are found in the brain, only L-serine is incorporated into proteins, while D-serine acts as a neuromodulator by co-activating NMDA receptors [Wolosker, 2006]. The reduction in serine could be due to increased protein synthesis, which has been shown for specific proteins such as BDNF, c-fos and various neurotransmitter receptors following rTMS [Chervyakov et al., 2015; Rodger et al., 2012]. Glycine is mostly synthesized *de novo* in the brain from serine, rather than taken up via the blood-brain barrier [Shank and Aprison, 1970], and accumulation of glycine in neurons requires the activity of the glycine transporter GlyT2 [Gomeza et al., 2003]. Thus, disruption of L-serine transport and/or diminished conversion of L-serine into glycine may contribute to the observed reduction in glycine. A key function for serine and glycine is to act as co-agonists for the NMDA receptor, which plays a central role in the long term plastic changes induced by high intensity rTMS[Vlachos et al., 2012], and may also contribute to LI-rTMS effects [Makowiecki et al., 2014; Rodger et al., 2012].

LI-rMS downregulates inositol and cholesterol - implications for calcium signalling and exocytosis

Inositol plays a key role as a precursor for inositol lipid and inositol phosphate syntheses, which are vital for signal transduction and intracellular calcium homeostasis [Wen et al., 2011]. A previous study showed that LI-rMS increases the levels of intracellular calcium in cortical neurons by release from intracellular stores, possibly via inositol-1,4,5-triphosphate (IP3) signalling [Grehl et al., 2015]. Inositol depletion as detected here may thus reflect the changes in intracellular signalling events induced by LI-rMS. Cholesterol was also decreased in our study. This lipid is not only important as a structural constituent of lipid rafts and cell membranes, but also modulates vesicle trafficking and exocytosis [Churchward et al., 2005; Lang et al., 2001; Zhang et al., 2009]. A recent study in ageing mice found that rTMS reduced cholesterol that accumulated with age [Wang et al., 2013]. This is important because cholesterol is associated with oxidative stress during normal aging [Cutler et al., 2004], and decreasing cholesterol levels can improve cognition in rats [Wang et al., 2013]. A decrease of cholesterol following rTMS and LI-rTMS, as suggested by our data, may thus contribute to the cognitive improvements observed following rTMS treatment of Alzheimer's patients [Hsu et al., 2015], and also in healthy volunteers [Miniussi and Ruzzoli, 2013].

Frequency-dependent metabolic changes

High and low frequency rTMS have different effects on neuronal circuits, with functional and genetic studies identifying distinct mechanisms in different neuronal cell types [Grehl et al., 2015; Pell et al., 2011]. Previous work using high intensity rTMS in anaesthetised cats demonstrated that metabolic changes were also frequency specific with increased glucose metabolism following high, but not low frequency stimulation [Valero-Cabré et al., 2007]. Our study provides a different approach, because we examined metabolic changes in a uniform

population of neuronal cells with an inhibitory phenotype. Thus our finding that the effects of LI-rMS are stronger with 1 Hz than with 10 Hz matches the inhibitory effect of 1 Hz that is consistently reported in animal and human literature [Chen et al., 1997; Maeda et al., 2000; Pell et al., 2011; Trippe et al., 2009]. However, because LI-rTMS does not induce action potentials, it remains unclear whether the metabolic changes we report are a direct consequence of the electromagnetic field, or whether they are secondary to the changes in excitability induced by rTMS.

CONCLUSION

Our study suggests that LI-rMS induces a depletion of metabolites consistent with an increase in GABA release as a result of higher spontaneous activity. While the B50 cell line is composed of cells that are electrically excitable and homogenous thus allowing for a targeted examination of the effects of LI-rMS on a defined cell population, the absence of defined neural circuits and other cellular contributors (e.g. excitatory neurons and glia) limits the degree to which our results can be extrapolated to the human brain. Nonetheless, the changes we describe provide novel insights into how LI-rTMS may modulate neural tissue and contribute to our understanding of the therapeutic application of electromagnetic brain stimulation.

ACKNOWLEDGEMENTS

The authors are grateful to Dr Alex Tang for advice and assistance with magnetic field measurements, to Dr Kartik Iyer for feedback on the manuscript, and to Mrs Marissa Penrose-Menz for support with artwork for figures.

REFERENCES

Abbiss H, Maker GL, Gummer J, Sharman MJ, Phillips JK, Boyce M, Trengove RD. 2012. Development of a non-targeted metabolomics method to investigate urine in a rat model of polycystic kidney disease. Nephrology 17:104-110.

Ahmed Z, Wieraszko A. 2008. The mechanism of magnetic field-induced increase of excitability in hippocampal neurons. Brain Research 1221:30-40.

Aldinucci C, Palmi M, Sgaragli G, Benocci A, Meini A, Pessina F, Pessina GP. 2000. The effect of pulsed electromagnetic fields on the physiologic behaviour of a human astrocytoma cell line. Biochimica et biophysica acta 1499:101-108.

Balassa T, Varro P, Elek S, Drozdovszky O, Szemerszky R, Vilagi I et al. 2013. Changes in synaptic efficacy in rat brain slices following extremely low-frequency magnetic field exposure at embryonic and early postnatal age. International Journal of Developmental Neuroscience 31:724-730.

Barker AT, Jalinous R, Freeston IL. 1985. Non-invasive magnetic stimulation of human motor cortex. Lancet 1:1106-1107.

Chen R, Classen J, Gerloff C, Celnik P, Wassermann EM, Hallett M, Cohen LG. 1997. Depression of motor cortex excitability by low-frequency transcranial magnetic stimulation. Neurology 48:1398-1403.

Capone F, Dileone M, Profice P, Pilato F, Musumeci G, Minicuci G, Ranieri F, Cadossi R, Setti S, Tonali PA, Di Lazzaro V. 2009. Does exposure to extremely low frequency magnetic fields produce functional changes in human brain? Journal of Neural Transmission 116:257-265.

Chervyakov A, Sinitsyn D, Chernyavsky A, Piradov M. 2015. Possible mechanisms underlying the therapeutic effects of transcranial magnetic stimulation. Frontiers in Human Neuroscience 9.

Churchward MA, Rogasevskaia T, Höfgen J, Bau J, Coorssen JR. 2005. Cholesterol facilitates the native mechanism of Ca2+-triggered membrane fusion. Journal of Cell Science 118:4833-4848.

Cutler RG, Kelly J, Storie K, Pedersen WA, Tammara A, Hatanpaa K, Troncoso JC, Mattson MP. 2004. Involvement of oxidative stress-induced abnormalities in ceramide and cholesterol metabolism in brain aging and Alzheimer's disease. Proceedings of the National Academy of Sciences of the United States of America 101:2070-2075.

Davey KR, Riehl M. 2006. Suppressing the surface field during transcranial magnetic stimulation. Biomedical Engineering, IEEE Transactions on 53:190-194.

Di Lazzaro V, Capone F, Apollonio F, Borea PA, Cadossi R, Fassina L, Grassi C, Liberti M, Paffi A, Parazzini M and others. 2013. A Consensus Panel Review of Central Nervous System Effects of the Exposure to Low-Intensity Extremely Low-Frequency Magnetic Fields. Brain Stimulation 6:469-476.

George MS, Lisanby SH, Avery D, et al. 2010. Daily left prefrontal transcranial magnetic stimulation therapy for major depressive disorder: A sham-controlled randomized trial. Archives of General Psychiatry 67:507-516.

Gomeza J, Ohno K, Hülsmann S, Armsen W, Eulenburg V, Richter DW, Laube B, Betz H. 2003. Deletion of the Mouse Glycine Transporter 2 Results in a Hyperekplexia Phenotype and Postnatal Lethality. Neuron 40:797-806.

Grehl S, Viola HM, Fuller-Carter PI, Carter KW, Dunlop SA, Hool LC, Sherrard RM, Rodger J. 2015. Cellular and Molecular Changes to Cortical Neurons Following Low Intensity Repetitive Magnetic Stimulation at Different Frequencies. Brain Stimulation 8:114-123.

Hoffman RE, Boutros NN, Hu S, Berman RM, Krystal JH, Charney DS. 2000. Transcranial magnetic stimulation and auditory hallucinations in schizophrenia. Lancet 355:1073-1075.

Hsu W-Y, Ku Y, Zanto TP, Gazzaley A. 2015. Effects of noninvasive brain stimulation on cognitive function in healthy aging and Alzheimer's disease: a systematic review and meta-analysis. Neurobiology of Aging 36:2348-2359.

International Commission on Non-Ionizing Radiation Protection (ICNIRP). 1998. Guidelines for limiting exposure to time-varying electric, magnetic, and electromagnetic fields (up to 300 GHz). Health Phys. 74:494-522.

Kumar A, Bachhawat AK. 2012. Pyroglutamic acid: throwing light on a lightly studied metabolite. Current Science (00113891) 102:288-297.

Lang T, Bruns D, Wenzel D, Riedel D, Holroyd P, Thiele C, Jahn R. 2001. SNAREs are concentrated in cholesterol-dependent clusters that define docking and fusion sites for exocytosis.

Li C-T, Chen M-H, Juan C-H, Huang H-H, Chen L-F, Hsieh J-C, Tu P-C, Bai Y-M, Tsai S-J, Lee Y-C and others. 2014. Efficacy of prefrontal theta-burst stimulation in refractory depression: a randomized sham-controlled study. Brain 137:2088-2098.

Lipton RB, Dodick DW, Silberstein SD, Saper JR, Aurora SK, Pearlman SH, Fischell RE, Ruppel PL, Goadsby PJ. 2010. Single-pulse transcranial magnetic stimulation for acute treatment of migraine with aura: a randomised, double-blind, parallel-group, sham-controlled trial. The Lancet. Neurology 9:373-380.

Maeda F, Keenan JP, Tormos JM, Topka H, Pascual-Leone A. 2000. Modulation of corticospinal excitability by repetitive transcranial magnetic stimulation. Clinical neurophysiology : official journal of the International Federation of Clinical Neurophysiology 111:800-805.

Makowiecki K, Harvey AR, Sherrard RM, Rodger J. 2014. Low-Intensity Repetitive Transcranial Magnetic Stimulation Improves Abnormal Visual Cortical Circuit Topography and Upregulates BDNF in Mice. The Journal of Neuroscience 34:10780-10792.

Manikonda PK, Rajendra P, Devendranath D, Gunasekaran B, Channakeshava, Aradhya RS et al. 2007. Influence of extremely low frequency magnetic fields on Ca2+ signaling and NMDA receptor functions in rat hippocampus. Neuroscience Letters 413:145-149.

Mantovani A, Simpson HB, Fallon BA, Rossi S, Lisanby SH. 2010. Randomized sham-controlled trial of repetitive transcranial magnetic stimulation in treatment-resistant obsessive–compulsive disorder. The International Journal of Neuropsychopharmacology 13:217-227.

Martiny K, Lunde M, Bech P. 2010. Transcranial low voltage pulsed electromagnetic fields in patients with treatment-resistant depression. Biological psychiatry 68:163-169.

Miniussi C, Ruzzoli M. 2013. Chapter 56 - Transcranial stimulation and cognition. In: Andres ML, Mark H (eds.). Handbook of Clinical Neurology: Elsevier. pp 739-750.

Müller-Dahlhaus F, Vlachos A. 2013. Unraveling the cellular and molecular mechanisms of repetitive magnetic stimulation. Frontiers in Molecular Neuroscience 6:50.

Navarro EA, Gomez-Perretta C, Montes F. 2016. Low intensity magnetic field influences short-term memory: A study in a group of healthy students. Bioelectromagnetics 37:37-48.

O'Reardon JP, Solvason HB, Janicak PG, Sampson S, Isenberg KE, Nahas Z, McDonald WM, Avery D, Fitzgerald PB, Loo C and others. 2007. Efficacy and Safety of Transcranial Magnetic Stimulation in the Acute Treatment of Major Depression: A Multisite Randomized Controlled Trial. Biological Psychiatry 62:1208-1216.

Pell GS, Roth Y, Zangen A. 2011. Modulation of cortical excitability induced by repetitive transcranial magnetic stimulation: influence of timing and geometrical parameters and underlying mechanisms. Progress in neurobiology 93:59-98.

Plewnia C, Reimold M, Najib A, Reischl G, Plontke SK, Gerloff C. 2007. Moderate therapeutic efficacy of positron emission tomography-navigated repetitive transcranial magnetic stimulation for chronic tinnitus: a randomised, controlled pilot study. Journal of Neurology, Neurosurgery & Psychiatry 78:152-156.

Rodger J, Mo C, Wilks T, Dunlop SA, Sherrard RM. 2012. Transcranial pulsed magnetic field stimulation facilitates reorganization of abnormal neural circuits and corrects behavioral deficits without disrupting normal connectivity. FASEB journal : official publication of the Federation of American Societies for Experimental Biology 26:1593-1606.

Rohan ML, Yamamoto RT, Ravichandran CT, Cayetano KR, Morales OG, Olson DP, Vitaliano G, Paul SM, Cohen BM. 2014. Rapid Mood-Elevating Effects of Low Field Magnetic Stimulation in Depression. Biological Psychiatry 76:186-193.

Rudiak D, Marg E. 1994. Finding the depth of magnetic brain stimulation: a re-evaluation. Electroencephalography and Clinical Neurophysiology/Evoked Potentials Section 93:358-371.
Shahbazi-Gahrouei D, Shiri L, Alaei H, Naghdi N. 2016. The effect of continuous ELF-MFs on the level of 5-HIAA in the raphe nucleus of the rat. Journal of Radiation Research doi:10.1093/jrr/rrv093.
Shank RP, Aprison MH. 1970. The metabolism in vivo of glycine and serine in eight areas of the rat central nervous system. Journal of Neurochemistry 17:1461-1475.
Shupak NM, Prato FS, Thomas AW. 2004. Human exposure to a specific pulsed magnetic field: effects on thermal sensory and pain thresholds. Neuroscience letters 363:157-162.
Terao Y, Ugawa Y. 2002. Basic Mechanisms of TMS. Journal of Clinical Neurophysiology 19:322-343.
Trippe J, Mix A, Aydin-Abidin S, Funke K, Benali A. 2009. θ burst and conventional low-frequency rTMS differentially affect GABAergic neurotransmission in the rat cortex. Experimental brain research. Experimentelle Hirnforschung. Expérimentation cérébrale 199:411-421.
Valero-Cabré A, Payne B, Pascual-Leone A. 2007. Opposite impact on 14C-2-deoxyglucose brain metabolism following patterns of high and low frequency repetitive transcranial magnetic stimulation in the posterior parietal cortex. Experimental Brain Research 176:603-615.
Valero-Cabré A, Payne BR, Rushmore J, Lomber SG, Pascual-Leone A. 2005. Impact of repetitive transcranial magnetic stimulation of the parietal cortex on metabolic brain activity: a 14C-2DG tracing study in the cat. Experimental brain research. Experimentelle Hirnforschung. Expérimentation cérébrale 163:1-12.
Vlachos A, Müller-Dahlhaus F, Rosskopp J, Lenz M, Ziemann U, Deller T. 2012. Repetitive magnetic stimulation induces functional and structural plasticity of excitatory postsynapses in mouse organotypic hippocampal slice cultures. The Journal of neuroscience : the official journal of the Society for Neuroscience 32:17514-17523.
Walleczek J, Budinger TF. 1992. Pulsed magnetic field effects on calcium signaling in lymphocytes: dependence on cell status and field intensity. FEBS letters 314:351-355.
Walsh V, Pascual-Leone A. 2003. Transcranial magnetic stimulation: a neurochronometrics of mind: MIT press Cambridge, MA.
Wang H, Geng Y, Han B, Qiang J, Li X, Sun M, Wang Q, Wang M. 2013. Repetitive Transcranial Magnetic Stimulation Applications Normalized Prefrontal Dysfunctions and Cognitive-Related Metabolic Profiling in Aged Mice. PLoS ONE 8:e81482.
Wen PJ, Osborne SL, Meunier FA. 2011. Dynamic control of neuroexocytosis by phosphoinositides in health and disease. Progress in Lipid Research 50:52-61.
Westergaard N, Varming T, Peng L, Sonnewald U, Hertz L, Schousboe A. 1993. Uptake, release and metabolism of alaume in neurons and astrocytes in primary cultures. Journal of Neuroscience Research 35:540-545.
Wolosker H. 2006. D-Serine Regulation of NMDA Receptor Activity. Science Signaling 2006:pe41-pe41.
Yang G, Ren Z, Mei YA. 2015. Exposure to 50 Hz magnetic field modulates GABAA currents in cerebellar granule neurons through an EP receptor-mediated PKC pathway. Journal of Cellular and Molecular Medicine 19:2413-2422.
Zhang J, Xue R, Ong W-Y, Chen P. 2009. Roles of Cholesterol in Vesicle Fusion and Motion. Biophysical Journal 97:1371-1380.
Zhang X, Liu X, Pan L, Lee I. 2010. Magnetic fields at extremely low-frequency (50 Hz, 0.8 mT) can induce the uptake of intracellular calcium levels in osteoblasts. Biochemical and Biophysical Research Communications 396:662-666.

FIGURE LEGENDS

Figure 1.Stimulation equipment. A,B: Photographs of the *in vitro* stimulation coils used in this study. Views are from the side (A) and top (B). The coils were situated at a distance of 2.8 mm from the bottom of the culture well because of the thickness of the coverplate and base of the culture dish.C: heatmap showing the measured change in magnetic field for a single pulse (dB/dT) when 6 coils are placed in a 6-well plate arrangement. Note the lack of overlap of magnetic field between the coils/wells of the plates.

Figure 2. Principal component analysis score plot of intracellular metabolites from GC-MS analysis of cells stimulated with LI-rMS at 1 Hz (n=4), 10 Hz (n=6) and unstimulated controls (n=6).

Figure 3. TCA cycle. Modified TCA cycle showing effects of LI-rMS on metabolic profile of B50 cells. Metabolites highlighted in yellow were significantly reduced in B50 cells following 1 and/or 10 Hz LI-rMS, compared to control B50 cells. The level of glucose (highlighted in green) was measured in our experiments and found to be unchanged by LI-rMS. The observed changes are proposed to result from increased *de novo* GABA synthesis (pathway a) that results in depletion of TCA cycle intermediates and precursors (pathways b, c, d).

Table 1. Intracellular metabolites identified by GC-MS and PCA as contributing the most to the variance between unstimulated controls and cells stimulated at 1 or 10 Hz and the fold change observed between stimulated cells and controls 1 Hz (n=4), 10 Hz (n=6) and unstimulated controls (n=6). Statistical significance was determined using a one-way ANOVA with Tukey's post-hoc test and is indicated as * = $p \leq 0.05$; ** = $p \leq 0.01$.

Table 1(on next page)

Fold change of metabolites following magnetic stimulation

Intracellular metabolites identified by GC-MS and PCA as contributing the most to the variance between unstimulated controls and cells stimulated at 1 or 10 Hz and the fold change observed between stimulated cells and controls 1 Hz (n=4), 10 Hz (n=6) and unstimulated controls (n=6). Statistical significance was determined using a one-way ANOVA with Tukey's post-hoc test and is indicated as * = $p \leq 0.05$; ** = $p \leq 0.01$.

Metabolite	Fold change (1Hz)	Fold change (10 Hz)	F-statistic
Amino acids			
Alanine	0.625**	0.873	6.477
Aspartate	0.322*	0.619	3.846
Glycine	0.570**	0.761**	19.162
Isoleucine	0.599**	0.753*	7.835
Phenylalanine	0.379**	0.477**	10.710
Serine	0.389**	0.656*	15.784
Threonine	0.606**	0.764*	11.286
Valine	0.942	0.956	0.064
Carbohydrates			
Fructose	0.638	0.958	1.788
Galactose	0.629	0.948	1.149
Glucose	0.858	0.938	0.161
Other metabolites			
Carbonic acid, 4- methylphenyl phenyl ester	1.268	1.267	2.021
Cholesterol	0.713**	0.831*	8.909
Glycerol-3-phosphate	0.801	0.798	4.155
Glycylglutamic acid	0.526**	0.693**	26.740
Inositol	0.563**	0.742	7.881
Pyroglutamate	0.531**	0.727*	9.603
Succinate	0.640**	0.803*	11.461

Table 1: Fold change between intracellular metabolites of cells stimulated at 1 and 10 Hz vs control. * $p \leq 0.05$, ** $p \leq 0.01$

Figure 1

Photographs showing equipment used for magnetic stimulation of cells

Stimulation equipment. A,B: Photographs of the *in vitro* stimulation coils used in this study. Views are from the side (A) and top (B). The coils were situated at a distance of 2.8 mm from the bottom of the culture well because of the thickness of the coverplate and base of the culture dish.C: heatmap showing the measured change in magnetic field for a single pulse (dB/dT) when 6 coils are placed in a 6-well plate arrangement. Note the lack of overlap of magnetic field between the coils/wells of the plates.

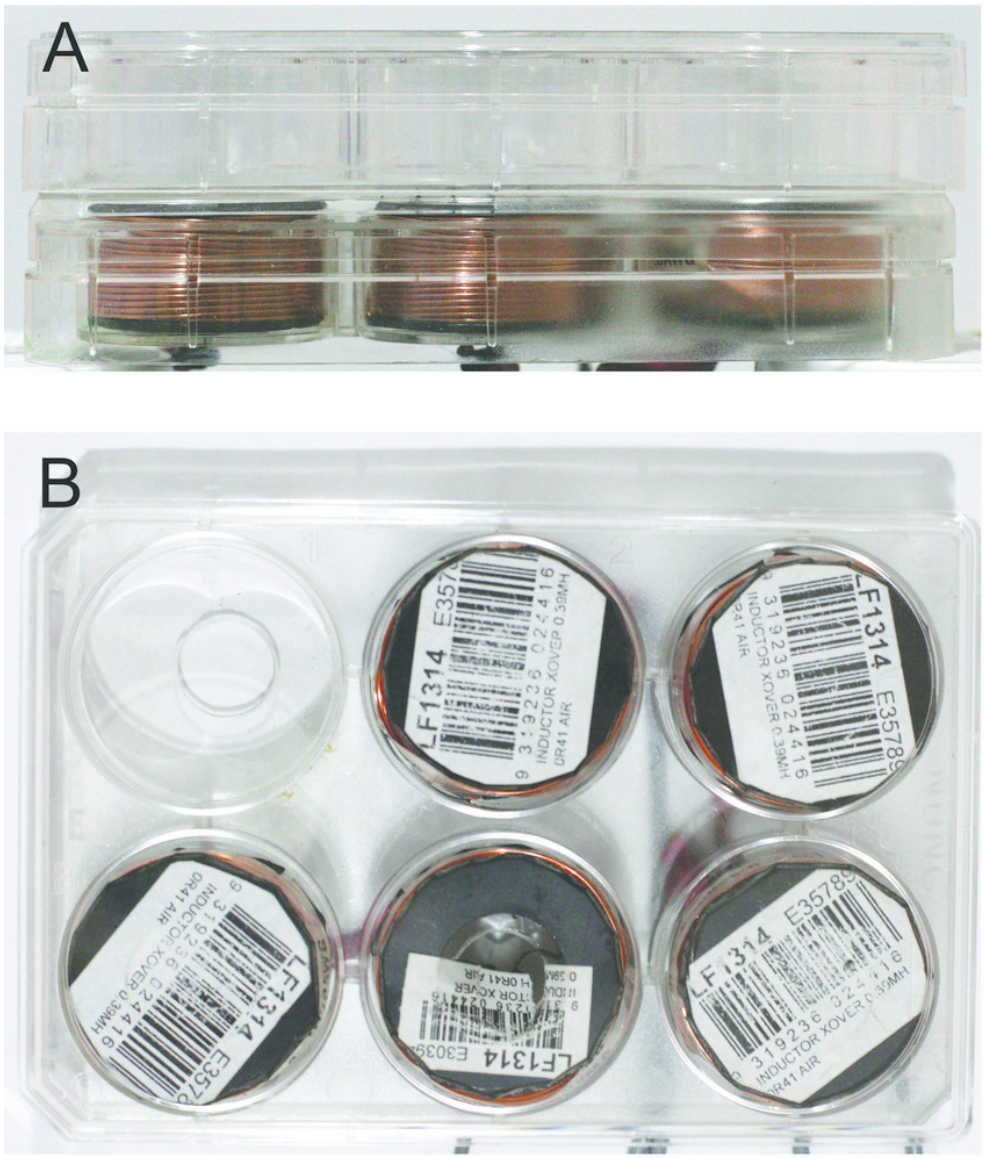

PeerJ Preprints | https://doi.org/10.7287/peerj.preprints.26446v1 | CC BY 4.0 Open Access | rec: 19 Jan 2018, publ: 19 Jan 2018

Figure 2

Principal components analysis of metabolites

Principal component analysis score plot of intracellular metabolites from GC-MS analysis of cells stimulated with LI-rMS at 1 Hz (n=4), 10 Hz (n=6) and unstimulated controls (n=6).

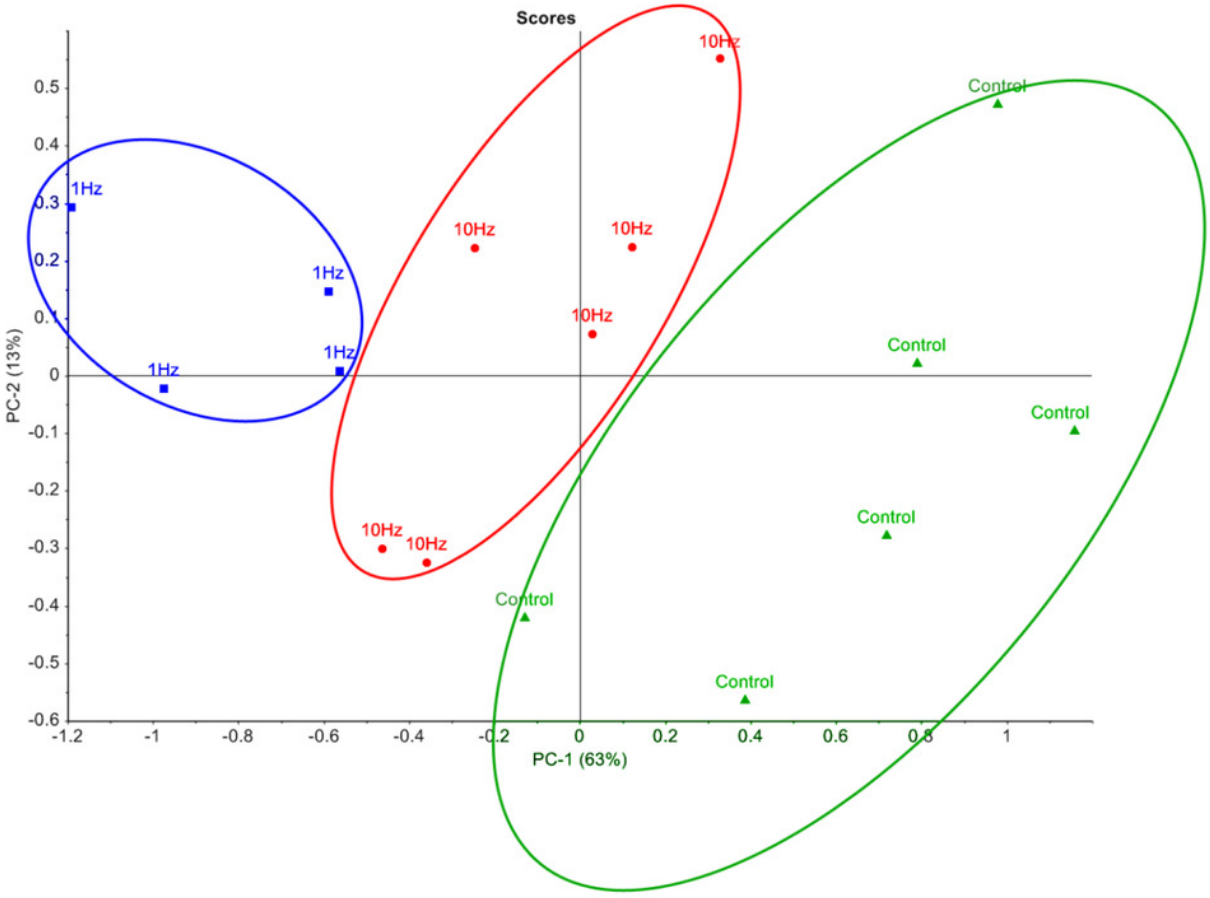

Figure 3

Diagram of TCA cycle highlighting changes observed in our study

TCA cycle. Modified TCA cycle showing effects of LI-rMS on metabolic profile of B50 cells. Metabolites highlighted in yellow were significantly reduced in B50 cells following 1 and/or 10 Hz LI-rMS, compared to control B50 cells. The level of glucose (highlighted in green) was measured in our experiments and found to be unchanged by LI-rMS. The observed changes are proposed to result from increased *de novo* GABA synthesis (pathway a) that results in depletion of TCA cycle intermediates and precursors (pathways b, c, d).

PeerJ Preprints | https://doi.org/10.7287/peerj.preprints.26446v1 | CC BY 4.0 Open Access | rec: 19 Jan 2018, publ: 19 Jan 2018